



# DYNAMIC ANALYSIS AND ATTITUDE CONTROL OF COAXIAL DUAL-ROTOR DUCTED AIRCRAFT

<sup>1</sup>JIA QINGXUAN, <sup>2</sup>LI TONG, <sup>3</sup>CHEN GANG

<sup>1</sup>Prof. of School of Automation, Beijing University of Posts and Telecommunications, Beijing, China

<sup>2</sup>Doctor of School of Automation, Beijing University of Posts and Telecommunications, Beijing, China

<sup>3</sup>Doctor of School of Automation, Beijing University of Posts and Telecommunications, Beijing, China

E-mail: <sup>1</sup>[qingxuan@bupt.edu.cn](mailto:qingxuan@bupt.edu.cn), <sup>2</sup>[bupt.litong@gmail.com](mailto:bupt.litong@gmail.com), <sup>3</sup>[buptcg@gmail.com](mailto:buptcg@gmail.com)

## ABSTRACT

A method of dynamic modeling and attitude control method for coaxial dual-rotor ducted aircraft is proposed. Based on aerodynamic analysis of the aircraft, the force status of the aircraft is obtained. By using the Newton-Euler equations, the dynamic model of the aircraft is built up, which is simplified to achieve a linear model at the hover state of the aircraft. Finally, the incremental PID controllers are designed to control the aircraft attitude at the hover state, which are proved efficiently to keep the aircraft attitude steady by the simulation and experiment results.

**Keywords:** *Coaxial Dual-rotor Ducted Aircraft; Dynamic Model; Incremental PID Controller*

## 1. INTRODUCTION

Ducted aircraft is a new type of aircraft developing rapidly in recent years, which is widely applied in areas of information investigation, environmental testing and geological survey. The ducted aircraft takes the characteristics of rotor aircraft and fixed-wing aircraft into account to achieve vertical take-off and landing, hovering flight, as well as high-speed forward flight. The duct on the aircraft is taken as annular wing to provide additional lift when the aircraft flies forward, which brings high flexibility and adaptability for the ducted aircraft. Meanwhile, the duct increases the concealment and security of the aircraft.

At present, many countries and organizations have taken research on ducted aircraft. The iSTAR [1] developed by United Airlines, Inc. is representative, as well as the micro air vehicle (MAV) [2] presided by Defense Advanced Research Projects Agency (DARPA). The "Fantail" ducted fan unmanned aerial vehicle (UAV) [3] manufactured in Singapore and MAV [4] exploited by the center for complex automated systems (CASYS) laboratory in University of Bologna also show good performance. A lot of works have also been done in China, such as the aerodynamics analysis and the wind tunnel experiments on ducted aircraft made by Nanjing University of Aeronautics and Astronautics, and the single rotor ducted UAV

researched by Harbin Institute of Technology. In preferences [1-4, 6], the ducted aircrafts have the structure of single rotor, deflector and control surfaces. These aircraft rely on the deflector to offset the reverse torque of the propeller and control the aircraft attitude with control surfaces, while the structure is too complex. A kind of ducted aircraft with the same proposed structures except deflector is designed by CASYS Laboratory, which can offset the reverse torque of the propeller with additional angles of control surfaces. But the design increases the complexity of the controller.

Based on the study of the research results on ducted aircraft, a motor-driven coaxial dual-rotor ducted aircraft is proposed in this paper. Coaxial propeller is designed to offset the reverse torque, and monolayer control surfaces are used in this design to control aircraft attitude, which simplify the structure and controller of the aircraft in a certain extent. Then aerodynamic characteristics of coaxial dual-rotor ducted aircraft are analyzed, and the dynamics model is built up, which is linearized to obtain the motion equations of the aircraft at hover state. Finally the incremental PID controller is put forward to achieve stable attitude control of the aircraft.

## 2. STRUCTURE AND AERODYNAMIC CHARACTERISTICS OF COAXIAL DUAL-ROTOR DUCTED AIRCRAFT

### 2.1 Structure of Coaxial Dual-rotor Ducted Aircraft

The structure of coaxial dual-rotor ducted aircraft is shown schematically as Figure 1, which consists of upper centrosome, ducted, propellers, lower centrosome, control surfaces and landing gear. The power unit and the propeller fan are installed on upper centrosome, while information collection devices can also be installed there, such as a camera. The propellers are composed of two propellers connected with two coaxial motors, which have the same pattern and rotate in the same direction. The two propellers have converse twist angle to offset the reverse torque. The duct is assembled around the propellers. Attitude measurement system and flight control system are assigned in the lower centrosome, and four control surfaces are attached there, too. The landing gear is at the bottom of the aircraft for the buffer to shocks.

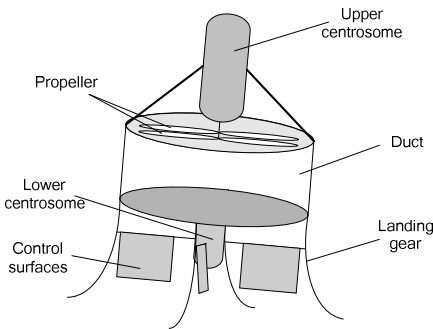


Figure 1 Schematic Diagram of Coaxial Dual-rotor Ducted Aircraft

When coaxial dual-rotor ducted aircraft takes off for a flight, lift is produced by the propeller rotation. The inverse torque can be offset because the propellers have converse twist angles. The control surfaces are arranged at the export of the duct. When air flows through, lift and drag generated by control surfaces change with angles of the control surfaces to control flight torque. The flight data are collected by the attitude measurement system and delivered to controller at any time in the flight, so that the angles of control surfaces can be adjusted real-time to achieve attitude control.

### 2.2 The Aerodynamic Analysis of Coaxial Dual-rotor Ducted Aircraft

The aerodynamic affected on the ducted aircraft is consist of lift generated by propeller, momentum drag, aerodynamic generated by duct, aerodynamic generated by control surfaces and gravity, which is shown as Figure 2.

In order to describe the aircraft conveniently, inertial coordinate system  $\Sigma_A$  and body coordinate system  $\Sigma_B$  are built up.  $\Sigma_A$  is represented by  $O_A x_0 y_0 z_0$ , where  $x_0$  points to north,  $z_0$  points to the earth, and  $y_0$  is generated by the right-handed rule.  $\Sigma_B$  is represented by  $O_B x_b y_b z_b$ , where  $x_b$  points to the direction of the flight,  $z_b$  points down along aircraft central axis, and  $y_b$  is generated by the right-handed rule, too. An intuitive representation of these coordinate systems is shown in Figure 2.

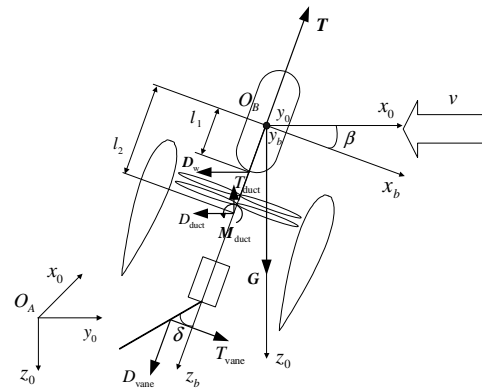


Figure 2 Aerodynamic Analysis of Coaxial Dual-rotor Ducted Aircraft

The attitude of  $\Sigma_B$  relative to  $\Sigma_A$  is described with ZYX - Euler angle as  $\Phi = (\gamma, \beta, \alpha)^T$ , while the angular velocity of  $\Sigma_B$  relative to  $\Sigma_A$  is described as  $\Omega = (p, q, r)^T$  in the same rule. Then the relationship between attitude angle and angular velocity is described as:

$$\Omega = A \dot{\Phi} \tag{1}$$

Wherein,  $A = \begin{bmatrix} 0 & -s\gamma & c\beta c\gamma \\ 0 & c\gamma & c\beta s\gamma \\ 1 & 0 & -s\beta \end{bmatrix}$ ,  $c$  represents

Cosine and  $s$  represents Sine.



**2.2.1 Lift generated by propeller**

Two propellers are used to offset the inverse torque, so the propellers generate lift only theoretically. The direction of the lift is along  $z_b$  and the value is represented by  $f$ .

The lift generated by propeller can be described with momentum theory as follow [8]:

$$f = 2\rho S \|v_i\|^2 \tag{2}$$

Wherein,  $\rho$  represents air density,  $S$  represents propeller blade area.  $v_i$  is the induced velocity of the propeller, the direction is the same as the positive direction of  $z_b$ .

**2.2.2 Momentum drag**

When the ducted aircraft flies, the relative velocity to the airflow is  $v = v_w + v_A$ , where  $v_w$  and  $v_A$  represent airflow velocity and flight velocity relative to the inertial coordinate system, respectively. The direction of airflow changes to the positive direction of  $z_b$  after it flows through the propeller. Then according to the Momentum theorem and Newton's law, the following equation can be concluded:

$$(-T - D_w) = \dot{m}v_\infty - \dot{m}v_w \tag{3}$$

The pull affected on the aircraft is  $T = -\dot{m}v_\infty$  [8], so the momentum drag is described:

$$D_w = \dot{m}v_w \tag{4}$$

$D_w$  affects on ducted lip [9], the direction of which is the same as the airflow.  $\dot{m}$  represents the mass flow, and can be solved by equation (5).

$$\dot{m} = \rho \|v_i\| S \tag{5}$$

$\|v_i\|$  represents the induced velocity which can be calculated with lift generated by propeller according to equation (2).

**2.2.3 Aerodynamic characteristics of duct**

The duct can be regarded as a kind of annular wing, which is generated by a specific airfoil surrounding the central axis of the aircraft around. The duct is installed around the propeller to decrease the turbulence when air flows over the blade tip of propeller. As a result the aerodynamic characteristics of propeller are improved. Meanwhile, the duct can provide additional lift when the aircraft flies a forward flight.

The lift and drag generated by the duct can be concluded as:

$$\left. \begin{aligned} T_{duct} &= \frac{1}{2} \rho S_d C_L(\chi) \|v\|^2 \\ D_{duct} &= \frac{1}{2} \rho S_d C_D(\chi) \|v\|^2 \end{aligned} \right\} \tag{6}$$

In equation (6),  $T_{duct}$  and  $D_{duct}$  represent the lift and drag generated by the duct, respectively.  $\rho$  is the air density, and  $S_d$  represents the effective area of the ducted.  $C_L(\chi)$  and  $C_D(\chi)$  concern with the angel of attack  $\chi$ , which represent lift coefficient and drag coefficient of the duct, respectively.

The resultant force affected on the duct is defined as  $F_{duct}$ , the action point of which locates inside the duct as Figure 2. The resultant moment is defined as  $M_{duct}$  which is generated by  $T_{duct}$  and  $D_{duct}$ .

**2.2.4 Aerodynamic characteristics of control surfaces**

Four control surfaces locate at the export of the duct, which are used to adjust aircraft attitude by controlling control surfaces angels. In the process, lift and drag are generated by the control surfaces, which are represented by  $T_{vane}$  and  $D_{vane}$ , respectively.

$$\left. \begin{aligned} T_{vane} &= \frac{1}{2} \rho S_v C_L(\delta) \|v_e\|^2 \\ D_{vane} &= \frac{1}{2} \rho S_v C_D(\delta) \|v_e\|^2 \end{aligned} \right\} \tag{7}$$

Wherein,  $v_e$  is the airflow velocity at the export of the duct, while  $S_v$  is the effective area of the control surfaces.  $C_L(\delta)$  and  $C_D(\delta)$  concern with the angle of attack  $\delta$ , which represent lift coefficient and drag coefficient of the control surfaces, respectively.

Excluding air compression, the airflow through the propeller and the export of the duct are the same in unit time. Then:

$$\rho S \|v_i\| = \rho S_e \|v_e\| \tag{8}$$

Wherein,  $S_e$  is the area of the export of the duct. On the basis of equation (8), the airflow velocity at the export of the duct  $\|v_e\|$  can be calculated with  $\|v_i\|$ .



$$\|v_c\| = \frac{S}{S_e} \|v_i\| \quad (9)$$

During attitude control of the aircraft, deflection angles of the four control surfaces are  $\delta_1 = \delta_r + \delta_y$ ,  $\delta_2 = \delta_p + \delta_y$ ,  $\delta_3 = \delta_r - \delta_y$ ,  $\delta_4 = \delta_p - \delta_y$ , where  $\delta_r$ ,  $\delta_p$ ,  $\delta_y$  represent roll, pitch and yaw angle, respectively. The resultant force affected on control surface is represented as  $F_{vane} = (F_{vanex}, F_{vanez})^T$  in  $\Sigma_B$ , while the resultant torque affected on control surface is  $M_{vane} = (M_{vx}, M_{vy}, M_{vz})^T$ .

### 2.2.5 Gravity

Gravity affects on barycenter of the aircraft, and is represented as  $G = (0, 0, mg)^T$  in inertial coordinate system.

## 3. THE DYNAMICS MODEL OF COAXIAL DUAL-ROTOR DUCTED AIRCRAFT

### 3.1 General Dynamics Equations based on Newton-Euler Equations

The centroid coordinate and relative velocity of the aircraft is defined as  $P = \{x, y, z\}^T$  and  $v = \{v_x, v_y, v_z\}^T$  expressed in  $\Sigma_A$ , respectively. Then according to Newton-Euler equations,

$$\begin{bmatrix} mI & 0 \\ 0 & J \end{bmatrix} \begin{bmatrix} \dot{v} \\ \dot{\Omega} \end{bmatrix} + \begin{bmatrix} 0 & 0 \\ 0 & \Omega \times J \Omega \end{bmatrix} = \begin{bmatrix} {}^A F \\ {}^B M \end{bmatrix} \quad (10)$$

Wherein,  ${}^A F$  is the resultant force affected on aircraft described in  $\Sigma_A$ , and  ${}^B M$  is the resultant torque affected on aircraft described in  $\Sigma_B$ .  $J$  represents inertial matrix of aircraft described in  $\Sigma_B$  as  $J = \text{diag}(J_x, J_y, J_z)$ . The equation  $J_x = J_y$  is satisfied, because the ducted aircraft is symmetric respect to plane  $o_b x_b z_b$  and  $o_b y_b z_b$ .

Considering  $\dot{P} = v$  and equations (1) and (10), the dynamics equations are concluded:

$$\left. \begin{bmatrix} \dot{P} \\ \dot{v} \\ \dot{\Omega} \end{bmatrix} = \begin{bmatrix} v \\ {}^A F/m \\ A^{-1} \Omega \\ J^{-1} ({}^B M - \Omega \times J \Omega) \end{bmatrix} \right\} \quad (11)$$

During the equation,  ${}^A F$  can be expressed as  ${}^A F = F_{duct} + D_w + R F_{vane} + G + R T$ , where  $R$  is the rotation matrix that can be calculated by equation (1).  ${}^B M$  can be expressed as  ${}^B M = M_{vane} + \varepsilon_1 \times R^{-1} D_w + \varepsilon_2 \times R^{-1} F_{duct} + M_{duct}$ , where  $R^{-1}$  is the inverse of the rotation matrix.  $\varepsilon_1$  and  $\varepsilon_2$  represent distance vectors from the action point of monument drag and drag generated by duct to the centroid of the aircraft, respectively. And the norms of the vectors are  $l_1$  and  $l_2$ .

### 3.2 Linearization of Dynamics Model at Hover State

In order to achieve stable attitude control for coaxial dual-rotor ducted aircraft at hover state, some assumptions are given out:

The absolute velocity of airflow is assumed as zero, then the velocity of the aircraft is represented as  $v_A = o(\varepsilon)$  at hover state, so the aerodynamic generated by duct can be neglected. The pitch and roll angles are represented as  $\beta = o(\varepsilon)$  and  $\alpha = o(\varepsilon)$ , respectively, then  $\sin \alpha = \alpha$  and  $\cos \alpha = 1$  can be obtained. As a result, the angular velocity of the ducted aircraft is expressed as  $\Omega = o(\varepsilon)$ , so  $\Omega \times J \Omega$  in equation (11) can be neglected.

At hover state, the angles of control surfaces change within small range, so the lift coefficient and drag coefficient can be approximated as  $C_L(\delta) = k_l \delta$  and  $C_D(\delta) = k_d \delta$  [6]. Define  $K_L = \rho S_v k_l v_c^2 / 2$  and  $K_D = \rho S_v k_d v_c^2 / 2$ , then  $T_{vane} = K_L \delta$  and  $D_{vane} = K_D \delta$  can be concluded. So  $F_{vane}$  can be represented as:

$$\left. \begin{aligned} F_{vanex} &= T_{vane2} + T_{vane4} = -2K_L \delta_p \\ F_{vanez} &= T_{vane1} + T_{vane3} = 2K_L \delta_r \\ F_{vanez} &= D_{vane1} + \dots + D_{vane4} = 2K_D (|\delta_r| + |\delta_p|) \end{aligned} \right\} \quad (12)$$

The angles of control surface are small enough so that the drag torque generated by control surfaces can be neglected. Then  $M_{vane}$  can be solved as:

$$\left. \begin{aligned} M_{vx} &= (T_{vane1} + T_{vane3}) l = -2K_L \delta_l \\ M_{vy} &= (T_{vane2} + T_{vane4}) l = -2K_L \delta_p \\ M_{vz} &= (T_{vane2} + T_{vane3} - T_{vane1} - T_{vane4}) n = 4K_L \delta_y n \end{aligned} \right\} \quad (13)$$

Wherein,  $l$  represents the distance between the action point of lift and centroid, and  $n$  represents the distance between the action point of lift and axis of  $z_b$ .

The velocity of aircraft is expressed as  $v_B = (v_{Bx}, v_{By}, v_{Bz})^T$  in  $\Sigma_B$ , the resultant force affected on the aircraft is expressed as  ${}^B F = ({}^B F_x, {}^B F_y, {}^B F_z)^T$  in  $\Sigma_B$ . Then the force and torque affected on the ducted aircraft are expressed as:

$$\left. \begin{aligned} {}^B F_x &= -\dot{m}v_{Bx} - 2K_L \delta_p - \beta mg \\ {}^B F_y &= -\dot{m}v_{By} + 2K_L \delta_r + \alpha mg \\ {}^B F_z &= -\dot{m}v_{Bz} - T + mg + 2K_D (|\delta_r| + |\delta_p|) \\ {}^B M_x &= \dot{m}v_{By}l - 2K_L \delta_r l \\ {}^B M_y &= -\dot{m}v_{Bx}l - 2K_L \delta_p l \\ {}^B M_z &= 4K_L \delta_y n \end{aligned} \right\} \quad (14)$$

In summary, the linearized motion equations of aircraft at hover state can be concluded.

Axial motion equations:

$$\begin{pmatrix} \dot{v}_{Bx} \\ \dot{\beta} \\ \dot{q} \end{pmatrix} = \begin{pmatrix} -\frac{\dot{m}}{m} & -g & 0 \\ 0 & 0 & 1 \\ -\frac{\dot{m}l}{J_y} & 0 & 0 \end{pmatrix} \begin{pmatrix} v_{Bx} \\ \beta \\ q \end{pmatrix} + \begin{pmatrix} -\frac{2K_L}{m} \\ 0 \\ -\frac{2K_L l}{J_y} \end{pmatrix} \delta_p \quad (15)$$

Transverse motion equations:

$$\begin{pmatrix} \dot{v}_{By} \\ \dot{\alpha} \\ \dot{p} \end{pmatrix} = \begin{pmatrix} -\frac{\dot{m}}{m} & g & 0 \\ 0 & 0 & 1 \\ \frac{\dot{m}l}{J_x} & 0 & 0 \end{pmatrix} \begin{pmatrix} v_{By} \\ \alpha \\ p \end{pmatrix} + \begin{pmatrix} \frac{2K_L}{m} \\ 0 \\ -\frac{2K_L l}{J_x} \end{pmatrix} \delta_r \quad (16)$$

Heading motion equations:

$$\begin{pmatrix} \dot{\gamma} \\ \dot{r} \end{pmatrix} = \begin{pmatrix} 0 & 1 \\ 0 & 0 \end{pmatrix} \begin{pmatrix} \gamma \\ r \end{pmatrix} + \begin{pmatrix} 0 \\ \frac{4K_L n}{J_z} \end{pmatrix} \delta_y \quad (17)$$

The air resistance can be neglected when the angles of control surfaces are very small, then the height motion equations can be concluded:

$$\begin{pmatrix} \dot{z} \\ \dot{v}_{Bz} \end{pmatrix} = \begin{pmatrix} 0 & 1 \\ 0 & -\frac{\dot{m}}{m} \end{pmatrix} \begin{pmatrix} z \\ v_{Bz} \end{pmatrix} + \begin{pmatrix} 0 \\ \frac{1}{m} \end{pmatrix} (mg - f) \quad (18)$$

#### 4. SIMULATION AND EXPERIMENT OF ATTITUDE CONTROL

Incremental PID control algorithm is used to achieve attitude adjustment at hover state for coaxial dual-rotor ducted aircraft, which is expressed as equation (19).

$$u(k) = u(k-1) + K_p [e(k) - e(k-1)] + K_i e(k) + K_d [e(k) - 2e(k-1) + e(k-2)] \quad (19)$$

Wherein,  $K_p$ ,  $K_i$ ,  $K_d$  represent scale coefficient, integral coefficient and differential coefficient, respectively.  $e(k)$  represents sampling deviation,  $k$  represents sampling number and  $u(k)$  represents output of the PID controller.

In part3, linearized motion equations of ducted aircraft are achieved at hover state, so that the independence of attitude control on three directions is realized. Then three kinds of PID controllers are built up to control the attitude independently, which achieve the aircraft stable control at hover state.

The stable attitude control of ducted aircraft at hover state aims at achieving dynamic equilibrium of pitch and roll angles in a small range. PID Controllers for pitch and roll angles control are designed respectively, where parameters of pitch angle controller are:  $K_{pp} = 3.1, K_{pd} = 2.5, K_{pi} = 2$ , the parameters for roll angle controller are:  $K_{rd} = 3.2, K_{rd} = 3, K_{ri} = 2$ .



Figure 3 Experiment of Attitude Control at Hover State

Table 1 Main Parameters of Coaxial Dual-rotor Ducted Aircraft

Parameters	Value
Quality/g	982
Load/g	300
Number of propellers	2
Diameter×thread pitch of propeller/ mm×mm	254×10.16
Minimum of duct inner diameter/ mm	260
Control cycle/ ms	50

In order to verify the efficiency of the PID controllers proposed above, experiments are taken out on a coaxial dual-rotor ducted aircraft. The attitude is controlled stably when the yaw angle is assigned at  $-8^\circ$ . The aircraft used in the experiment is shown as Figure 3, and the main parameters of the aircraft are listed in Table 1. The result is given out in Figure 4.

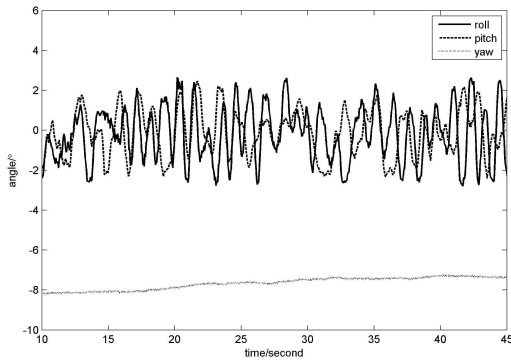


Figure 4 Three kinds of Attitude Angles during Attitude Control at Hover State

From Figure 4, it's seen that the yaw angle of the aircraft stays steady, which proves the structure of two propellers can offset the reverse torque efficiently. The pitch and roll angles achieve dynamic equilibrium between  $-2^\circ$  and  $2^\circ$  at hover point, which verifies the designed PID controller can achieve stable attitude control efficiently. The force affected on the aircraft is not homogeneous because of machining inaccuracy and assembling errors, that's the main reason why the pitch and roll angles waves. Seriously, it will cause asymmetry of lift generated by propellers, which will cause unstable yaw attitude.

Based on the experiment of stable attitude control for aircraft, research on response status of the controller is implemented. The response status of pitch angle is taken as research object, the actual changes of the pitch angle are measured when desired changes are input the controller. Both

Matlab simulation and flight experiment are carried out, and the comparison curves of the response status are shown as Figure 5. It is seen that the controller can follow the changes of the angle in good accuracy. Meanwhile, the controller responds to orders rapidly. In summary, the incremental PID controllers can adjust attitude angles in real-time when the attitude of the aircraft changes, the dynamic response characteristics of the controllers are confirmed well.

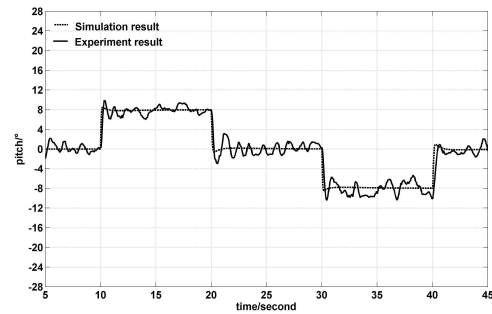


Figure 5 Comparisons between Simulation and Experimental Result of Pitch Angle Response Status

## 5. CONCLUSIONS

A kind of coaxial dual-rotor ducted aircraft is proposed in this paper, and the aerodynamic characteristics are analyzed. Then the dynamic model of the aircraft is built up based on Newton-Euler equations, which is linearized at hover state. With the linearized dynamic model, incremental PID controllers are designed for stable attitude control. By simulation and experiments, the attitude can be stably controlled in small angle range when the aircraft is in hover state. Meanwhile, the controller can adjust attitude angles in real-time with good dynamic response characteristics.

## REFERENCES:

- [1] Larry Lipera, Jason D Colbourne, and Mark B Tischler. "The micro craft iSTAR micro air vehicle: control system design and testing", *Proceedings of American Helicopter Society 57th Annual forum*, May 9-11, 2001, pp. 1998-2008.
- [2] Honeywell. Class I UAVs[EB/OL]. (2006-7-26) [2011-3-26]. <http://defenseupdate.com/products/h/honeywellmav.htm>.
- [3] Irving Tjin, Raymond Chia Kiah Nglan, and Kevin Chan. "Fan Tail flight controller design and flight testing", *Aerospace Technology Seminar 2007*, March, 2007, pp. 1-8.



- [4] L. Gentili, L. Marconi, and R. Naldi. "Experimental framework for a ducted-fan miniature aerial vehicle", *2009 American Control Conference*, June 10-12, 2009, pp. 4159-4164.
- [5] LI Jian-bo, and GAO Zheng. "Aerodynamical characteristics analysis of ducted fan", *Journal of Nanjing University of Aeronautics & Astronautics*. Vol.37, No.6, 2005, pp. 680-684.
- [6] LI Yuan-wei, WANG Chang-hong, YI Guo-xing, et al. "Robust control system design for a ducted fan unmanned aerial vehicle", *Electric Machines and Control*. Vol.14, No.9, 2010, pp. 81-87.
- [7] L. Marconi, R. Naldi, and A. Sala. "Modeling and analysis of a reduced complexity ducted MAV", *14th Mediterranean Conference on Control and Automation*, June 28-30, 2006, pp. 1-6.
- [8] Liu Peiqing. "The air propeller theory and its application", *Beihang University Press*, 2006, pp. 55-59.
- [9] Ignacio Guerrero, Kelly Londenberg, and Paul Gelhausen. "A powered lift aerodynamic analysis for the design of ducted fan UAVs", *2nd AIAA "Unmanned Unlimited" Systems, Technologies, and Operations-Aerospace*, September 15-18, 2003, pp. 1-8.
- [10] J. M. Pflimlin, P. Soueres, and T. Hamel. "Position control of a ducted fan VTOL UAV in cross-wind", *International Journal of Control*. Vol.80, No.5, 2007, pp. 666-683.
- [11] Richard Harris. "Investigation of control effectors for ducted fan VTOL UAVs", *Virginia Polytechnic Institute and State University*, 2007.